Fire Safety Journal, 10 (1986) 173 - 184

Structural Steel and Plane Frame Assemblies under Fire Action*

ACHIM RUBERT and PETER SCHAUMANN

Krupp Forschungsinstitut, Münchener Strasse 100, 43 Essen 1 (F.R.G.)

(Received September 6, 1985; in revised form February 7, 1986)

SUMMARY

By means of series of tests carried out on simply supported beams of standard rolled sections subjected to bending, fully analytically formulated calculation values were derived for the temperature-dependent stress–strain relationships of structural steel under fire action from normal temperature to 1000 °C.

Systematic series of investigations carried out on frame assemblies made up from rolled sections with high scale accuracy revealed the characteristic parameters influencing the critical temperatures. The analyses showed good-to-excellent agreement both for the temperature–displacement curves and for the critical temperatures, so that the integrity of the stress–strain relationships could also be verified for combined bending and compressive stress states and for stability-endangered assemblies.

The knowledge gained by way of experiment and computation furnished — in generalized terms — a basic concept for the simple and uniform assessment of the resistance to fire action of single elements and whole assemblies of structural steel subject mainly to bending stresses or endangered in stability. This allows the collapse temperatures of uniformly heated systems to be determined as a function of load utilization factor and system slenderness. These major parameters — load utilization factor and system slenderness ratio — are normal temperature design characteristics and can be determined using conventional methods.

*Submitted to Technical Committee 3 "Fire safety of steel structures" of the European Convention of Structural Steelwork. Meeting held in Helsinki in May, 1985.

0379-7112/86/$3.50

INTRODUCTION

In the past, national and international research activity into the load-bearing characteristics of structural steel constructions under fire action was restricted mainly to the study of single structural elements. The behaviour of whole constructions from the point of view of the interaction of single elements has not yet been investigated in great detail, and those investigations which have touched on the subject have as yet had no tangible effect on fire resistance design practice. There are obvious reasons for this. Full-scale tests on original steel structures (for example, see ref. 1) may allow general statements to be made but, because of the complex relationships involved, they permit only limited assessment of the load-bearing behaviour of single components. Technical constraints and costs make extensive series of tests with a view to systematic research unfeasible. This also applies to investigations carried out on sub-assemblies [2] on a scale of 1:1 under standard fire conditions (ISO 834). Small-scale model tests (scale 1:20) [3] can be carried out with much less outlay. The deformation figures at the moment of failure observed in such tests agree qualitatively with the deformations encountered in natural fire conditions. Quantitatively, however, the results of such small-scale model tests are not so readily transferable to real structures and do not lend themselves to generalization. Small-scale models (for example, see ref. 4) are also unsuitable for calibrating theoretical methods of investigation to be used in the design of original structures.

Methods of designing *steel frame constructions* subject to fire action are based mainly on the yield hinge theory [5]. The use of such methods, which under certain conditions

provide good approximations in design under normal temperatures, is problematic in the high temperature range because the stress–strain behaviour of structural steel at elevated temperatures is essentially different from that encountered at normal temperatures. Proof of integrity through comparisons in fire tests has not yet been furnished.

For *single bars*, e.g., columns, more discerning design methods are already in use [6, 7]. In these, however, it has become clear that the calculation values assumed for temperature-dependent behaviour differ widely in some cases. In particular, it has not been adequately demonstrated whether the knowledge gained from small-scale tensile tests is transferable to single elements or whole assemblies.

In the period 1981 to 1984, coordinated experimental and theoretical investigations, commissioned by the Studiengesellschaft für Anwendungstechnik von Eisen und Stahl e.V., and funded by the Federal Ministry for Research and Technology, were carried out in close cooperation between Krupp Forschungsinstitut, Essen [8], and the structural engineering department of Ruhr University, Bochum [9], to study the behaviour of structural steel and the load-bearing characteristics of single elements and frame constructions under the action of fire.

LARGE-SCALE MODEL TECHNIQUE

To allow systematic experimental investigations to be carried out at justifiable economic expense on whole constructions, a technique was developed with a view to researching the fire resistance behaviour of materials also subjected to external loads. This technique has been termed the large-scale model technique to distinguish it from the small-scale approach [10].

In contrast to the small-scale model, a large-scale model is a model which under all loading conditions offers strict similarity to the original in terms of stresses, strains, deformations and even load-bearing capacity. These requirements and a number of other considerations, such as the technical feasibility of the points of support and the points of load introduction, including force measurements, etc., led to the development of a model technique based on a scale of 1:4 to 1:6.

One major feature distinguishing these tests from conventional fire tests using oil burners is the use of a special electric resistance heating system, consisting of a number of 25 cm and 35 cm long semi-circular furnace shells of high-temperature-resistant insulating material with integrated heating conductors. The individual heating elements can be grouped as desired and arranged in a circle around the structural elements with enough space left in between to accommodate the expected deformations. The heat supply is controlled by computer, each ring element having its own control loop. Where necessary, several ring elements can be combined to form one heating segment. In the course of the tests using a uniform heating rate, however, it was found that separate control of each ring element was more suitable since it allowed even slight temperature gradients over the length of the structural member to be corrected at an early stage by the automatic control system.

The variable temperature field was not controlled on the basis of the gas temperature in the furnace (as is the case in the test furnaces of the materials testing institutes). The controlled quantity rather was the progression over time of the steel temperature $T(t)$ of the large-scale model, which was unprotected at all times. Thus, the fire exposure (e.g., *ISO 834*) and the temperature of the structural member are decoupled, and virtually any desired temperature/time curve can be realized. The effects of fire protection on the original structural member can therefore be taken indirectly into account through selection of a suitable heating rate. In addition, direct control of the rate at which the unprotected steel section is heated offers the advantage that no model-static problems derive from the effects of heat transfer and heat conduction in the gas, in the fire protection and in the structure itself.

TRANSIENT-STATE TESTS ON BEAMS SUBJECTED TO BENDING LOADS; TEMPERATURE-DEPENDENT STRESS–STRAIN RELATIONSHIPS DERIVED THEREFROM

The temperature-dependent behaviour of structural steel under simultaneous external

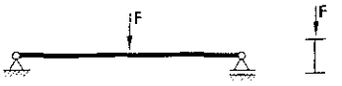

Fig. 1. The test specimen for the transient-state tests: a beam simply supported with a single load in the midspan.

and thermal loading has been studied up to now mainly on the basis of uniaxial tensile tests. Clear statements on whether the results can be applied to structural members, made of rolled sections for example, are not available.

Seventeen tests were carried out on simply supported beams (IPE 80 and IPE 120, St 37) with a single load being applied in the midspan (Fig. 1). The beams, under constant load, were heated uniformly along their entire length. The electronic temperature control system made it possible to achieve extremely uniform temperatures throughout the beam.

The parameters varied in the test series were the load utilization factor $1/\nu_u = F/F_u$ (between 0.05 and 0.85), which represents the ratio of actual load to ultimate load-bearing capacity at normal temperatures given by knowledge of the actual (measured) upper yield point $\beta_s = R_{eH}$, and the mean heating rate $\dot{T}_m$ (between 2.67 and 32 K min^{-1}). Tests WK 1 - WK 12 were conducted using IPE 80 sections, tests WK 13 - WK 15 using IPE 120 sections. Figure 2 shows, for tests WK 1 - WK 12, a comparison of midspan deformation behaviour at different heating rates.

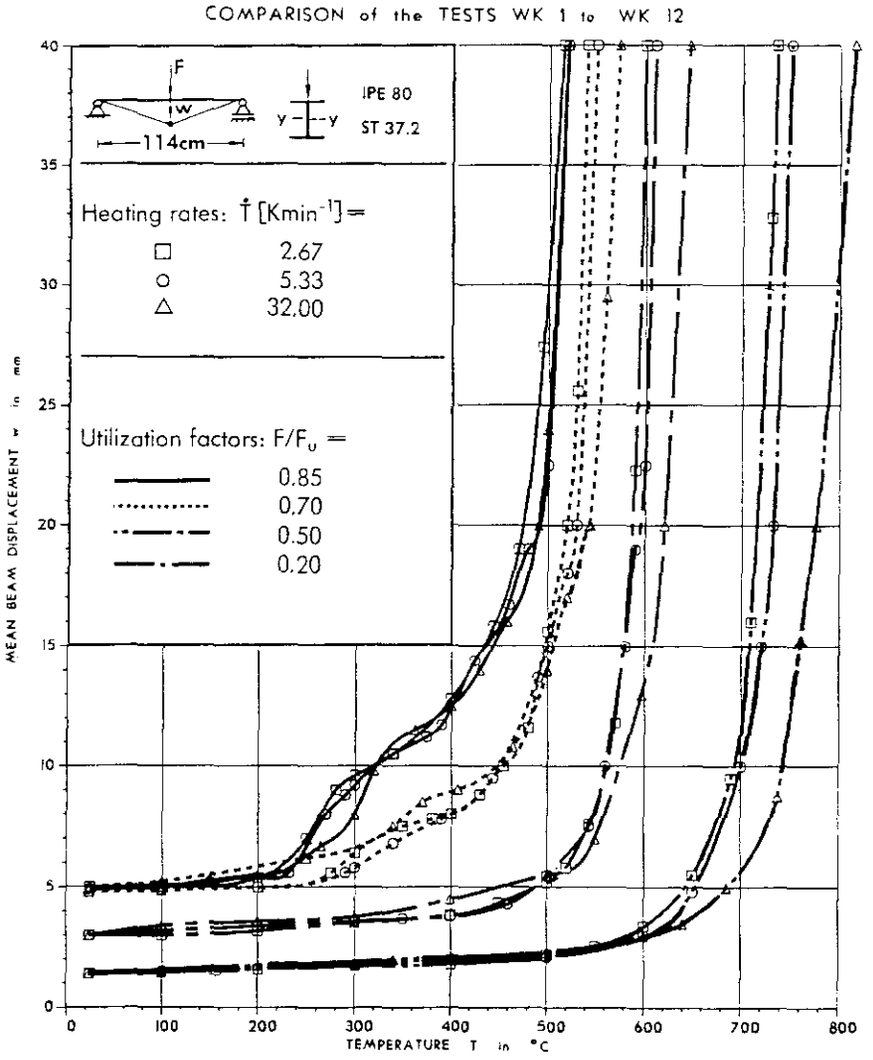

Fig. 2. Comparison of the temperature–displacement curves as functions of heating velocity $\dot{T}_m$ and utilization factor F/F_u.

The three mean heating rates T_m used were selected such that steel temperatures of 500 °C are reached after 15, 90 and 180 minutes. This covers the whole range of relevant heating rates for steel structures, also taking into account the effects of fire protections.

The measured temperature/deformation curves were used to obtain stress–strain calculation values. The point at which plastic failure occurred, as a result of the load-bearing capacity of the cross-section at midspan being reached, was used to determine the temperature-dependent yield point.

As a simplification the critical temperature crit T was taken as the steel temperature recorded when a midspan deformation in the beam of $l/60$ was reached. Formal application of the failure criterion of DIN 4102, Part 2, para 5.2.6 [11] on the limitation of the deformation rate

$$\frac{\Delta w(\text{cm})}{\Delta t(\text{min})} = \frac{l(\text{cm})^2}{9000h(\text{cm})} \qquad (1)$$

would lead to a slightly higher crit T compared with the $l/60$ criterion for heating rates $\dot{T}_m = 5.33\ \text{Kmin}^{-1}$ and a lower crit T for $\dot{T}_m = 32\ \text{Kmin}^{-1}$.

Figure 3 shows the critical temperatures crit T as a function of the load utilization factor $1/\nu_u$, the heating rate $\dot{T}_m$ and the section compared with temperature-dependent referred yields points $\bar{\beta}_s$. The test values for identical utilization factors and different heating rates lie close together. Both the DIN 4102 proposal [11] and the ECCS proposal [12] are very much on the safe side and therefore represent a conservative estimate of real behaviour. In contrast, the proposal for $\bar{\beta}_s(T)$ developed on the basis of the beam tests is very close to the measured values and represents a lower limit in terms of the effect of the heating rates under investigation in the relevant range.

Owing to the practically isothermal distribution of temperature over the cross-section and length of the beam, the purely thermally induced strains affect only the length variation of the beam, but not its deflection figure. The temperature midspan deformation curves measured in the test are therefore particularly suitable for the development of temperature-dependent stress–strain relationships, i.e., the relationship between stresses, stress-inducing strains and steel temperature.

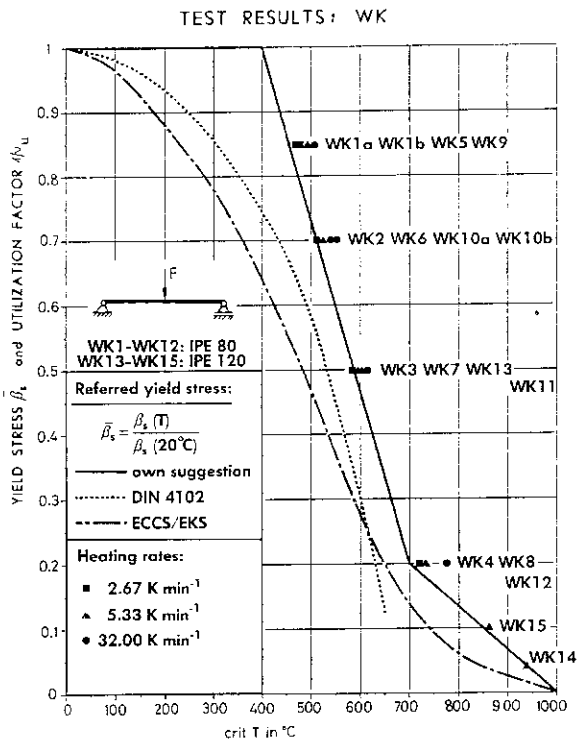

Fig. 3. The critical temperatures crit T as a function of the utilization factor $1/\nu_u$ and the heating velocity $\dot{T}_m$ in comparison to the temperature-dependent yield stress $\bar{\beta}_s$.

Furthermore, the selection of simple, statically determined beams makes for clearly defined support conditions and restraint-free beam deformations, and rules out all imponderables deriving from stability influences (initial deformations, etc.).

The complete stress–strain behaviour was derived numerically from the measured deformations. With a given constant load, the equilibrium between outer and inner bending moments

$$M^a(x) = M^i(x) = \int_A \sigma(\epsilon, T) \times z \times \mathrm{d}A \qquad (2)$$

was sought at each point on the beam in a first conditional equation. Using the Bernoulli hypothesis, this gave a plane strain condition for a specific stress condition. The curvature resulting from the strain condition was integrated to form a deflection figure which was to be brought into agreement with the value determined in the test in midspan in a second conditional equation.

In contrast to conventional specimens having homogeneous stress conditions, the stresses in the beams are variable over both

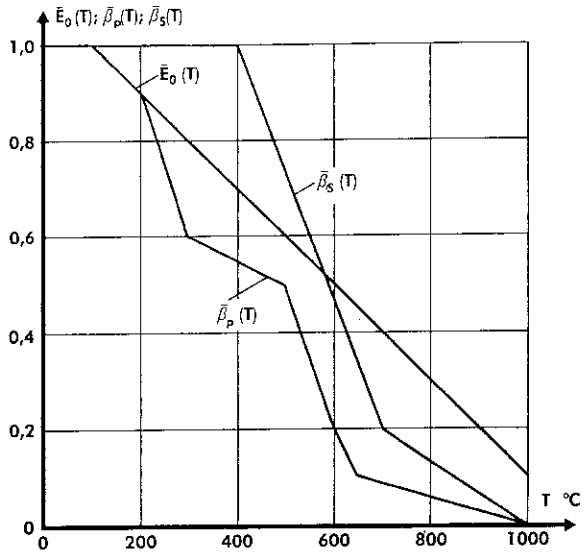

Fig. 4. The temperature-dependent initial modulus of elasticity E_0, elastic limit β_p and yield point β_s.

the longitudinal axis and the cross-section of the bar. The integration of the stress–strain conditions of the whole beam to eqn. (2) thus contains the entire spectrum of stress levels in the temperature range under investigation.

The results of these computations were the temperature dependence of the initial modulus of elasticity $E_0(T)$, the elastic limit $\beta_p(T)$ and the yield point $\beta_s(T)$, whose progression is shown in referred form in Fig. 4 as a function of steel temperature:

$$\bar{E}_0(T) = \frac{E_0(T)}{E_0(20\ ^\circ\mathrm{C})} \tag{3}$$

$$\bar{\beta}_p(T) = \frac{\beta_p(T)}{\beta_s(20\ ^\circ\mathrm{C})}$$

$$\bar{\beta}_s(T) = \frac{\beta_s(T)}{\beta_s(20\ ^\circ\mathrm{C})}$$

Using these characteristic values a mathematical formulation was selected as follows (Fig. 5): the function is characterized by an initially linear progression up to the elastic limit β_p; this is followed by an elliptical progression up to the yield point β_s; by formulating the transition from the elastic to the plastic region as an elliptical progression, the function $\sigma = f(\epsilon, T)$ becomes continuously differentiable. Thus, the tangent

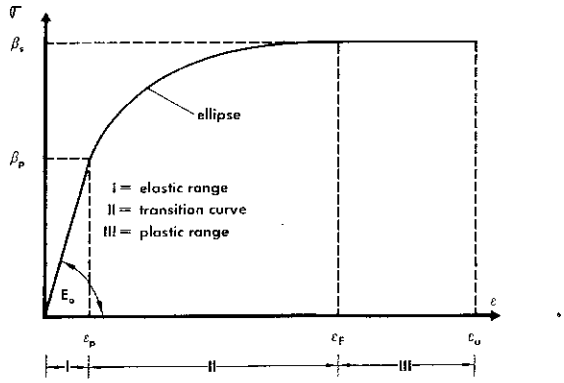

Fig. 5. The basic formulation of the stress–strain relationship of structural steel under fire action.

modulus E can be stated clearly as the first derivative for any desired strain.

Table 1 gives the analytical formulation of the σ-ϵ-stress-strain calculation values for structural steel. The yield strain ϵ_F and ultimate strain ϵ_u are assumed to be temperature-independent. Figure 6 shows, by way for example, the stress–strain behaviour for grade St 37 steel (β_s = 240 N/mm^2).

The agreement of the calculated temperature–displacement curves with the tests is good for the entire spectrum of utilization factors investigated. It should be noted that the overproportionate increase in deformation from about 200 °C onwards for the high utilization factors $F/F_u \geqslant 0.7$ is included in this temperature range as a result of the sharper fall in the referred elastic limit $\bar{\beta}_p$ compared with $\bar{E}_0$.

In summary, the temperature-dependent stress–strain relationships have the following properties:

— implicit allowance of creep effects for heating rates $2 \leqslant \dot{T} \leqslant 30$ K/min;

— suitable for rolled sections due to direct calibration in single element tests with fully defined thermal and mechanical boundary conditions;

— formulated completely analytically and continuously differentiable;

— linear temperature dependence in sections of the characteristic parameters E_0, β_p, β_s;

— description of pure material behaviour, excluding the effects of structural and geometrical imperfections.

A more detailed description of the development of the stress–strain relationships is given in ref. 15.

TABLE 1

The analytical formulation for the stress–strain relationship of structural steel under fire action, derived by transient-state tests with large-scale beam models

Range*	$\sigma(\epsilon, T) =$	$E(\epsilon, T) =$
I Elastic $0 \leqslant \epsilon \leqslant \epsilon_p$	$E_0(T)\epsilon$	$E_0(T)$
II Transition (elliptic) $\epsilon_p \leqslant \epsilon \leqslant \epsilon_F$	$\frac{b}{a}\sqrt{a^2 - (\epsilon_F - \epsilon)^2} + \beta_p(T) - c$ with $a^2 = \frac{E_0(T)(\epsilon_F - \epsilon_p)^2 + c(\epsilon_F - \epsilon_p)}{E_0(T)}$ $b^2 = E_0(T)(\epsilon_F - \epsilon_p)c + c^2$ $c = \frac{[\beta_s(T) - \beta_p(T)]^2}{2[\beta_p(T) - \beta_s(T)] + E_0(T)(\epsilon_F - \epsilon_p)}$	$\frac{b(\epsilon_F - \epsilon)}{a\sqrt{a^2 - (\epsilon - \epsilon_F)^2}}$
III Plastic $\epsilon_F \leqslant \epsilon \leqslant \epsilon_u$	$\beta_s(T)$	0

*With $\epsilon_p = \frac{\beta_p(T)}{E_0(T)}$, $\epsilon_F = 2\%$ and $\epsilon_u = 20\%$.

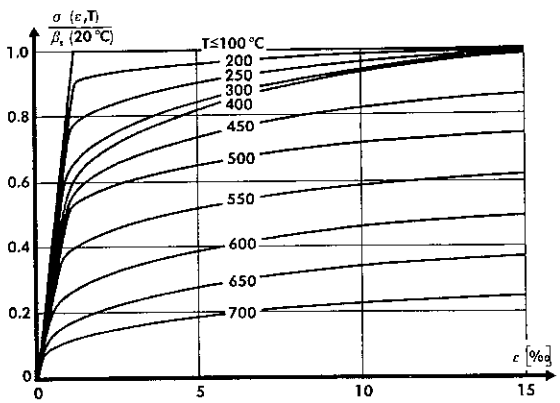

Fig. 6. The temperature-dependent stress–strain relationship of St 37.

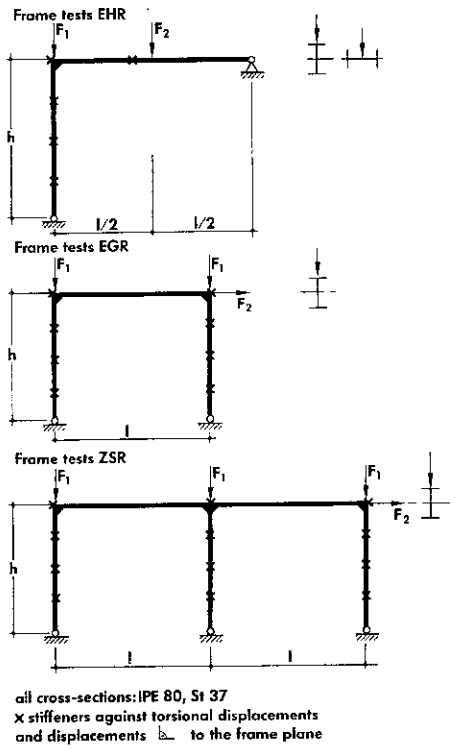

Fig. 7. Survey on frame test program.

LOAD-BEARING CHARACTERISTICS OF FRAME SYSTEMS

Figure 7 shows the static systems as well as the external loads of the frame configurations investigated. In the first test series (EHR) braced two-bar frames were tested which were heated completely and uniformly. In the various tests the load utilization factor and the slenderness ratio were varied. In the second and third test series, unbraced frames were investigated. The second series (EGR) dealt with simply supported frames, as are often encountered in design practice. The

TABLE 2

Test parameters and results of the frame tests

System	l (cm)	h (cm)	β_s (kN/cm²)	F_1 (kN)	F_2 (kN)	$1/\nu_u$	$\bar{\lambda}_{sys}$	crit T		Remarks
								Test (°C)	Calculation (°C)	
										fully heated:
EHR 1	119	117	39.5	56	14	0.38	0.33	600	632	
EHR 2	124	117	39.5	84	21	0.59	0.33	530	553	bending about the strong axis
EHR 3	124	117	38.2	112	28	0.82	0.33	475	462	
EHR 4	125	150	38.9	20	5	0.59	0.65	562	540	
(EHR 5)*	125	150	38.9	24	6	0.71	0.65	460	493	bending about the weak axis
(EHR 6)	125	150	38.9	27	6.7	0.79	0.65	523	437	
										bending about the strong axis:
EGR 1b	122	117	38.2	65	2.5	0.55	0.93	533	507	
EGR 1c	122	117	38.2	65	2.5	0.55	0.93	515	507	
EGR 2	122	117	38.5	40	1.6	0.34	0.93	612	599	
EGR 3	122	117	38.5	77	3.0	0.66	0.93	388	415	fully heated
EGR 4	122	117	41.2	77	3.0	0.63	0.96	424	439	
EGR 5	122	117	41.2	88	3.4	0.72	0.96	335	330	
EGR 6	122	117	41.2	88	3.4	0.72	0.96	350	330	
EGR 7/KR	122	117	32.0	68.5	2.6	0.65	0.84	454	441	
EGR 8/KR	122	117	38.5	77	3.0	0.70	0.89	464	404	cold beam
EGR 9/ΔT	122	117	41.2	88	3.4	0.72	0.96	38.7 min	37.5 min	temperature gradient in the beam
EGR 10/FP	120	113.5	43.2	82	3.1	0.63	0.98	609	613	realistic foot plate
										bending about the strong axis:
ZSR 1	120	118	35.5	74.0	2.85	0.60	0.94	547	525	
ZSR 2	120	118	38.0	84.5	3.25	0.66	0.97	479	483	partly heated
ZSR 3	120	118	43.2	68.5	2.64	0.50	1.03	574	584	

*( ) ≙ Frame partly in the plastic range already under normal temperature.

first frames were heated completely and uniformly, with the load utilization factor varying. Then, in supplementary tests, the effects of inhomogeneous temperature distributions and a practical column base configuration were investigated. In the third series, two-portal frames (ZSR) were tested with different load utilization factors. Only one portal of the frame was heated in order to investigate the stabilizing effect of (unheated) frame elements lying outside the fire compartment.

All columns in the model are secured by stiffener elements against torsional displacement and out-of-plane deformation by adequately spaced stiffener elements. The location of the stiffeners is also shown in Fig. 7.

The dimensions and the loadings used in all the individual tests are shown in Table 2. The same table contains actual (measured in tensile tests) yield points at normal temperature, used to determine the utilization factor $1/\nu_u = F/F_u$, taking into account the calculated load-bearing capacity under normal temperatures. The load-bearing capacity at normal temperatures was determined using the 2nd order theory, taking into account plastification of cross-sections and geometric non-linearities. The load utilization factor $1/\nu_u$ thus defined is largely independent of national, variable codes with regard to design loads.

Table 2 also contains measured and calculated critical temperatures.

For the theoretical simulation of the large-scale frame tests a numerical method was used which was prepared in ref. 13. It is an incrementally formulated finite element method for structural assemblies based on the displacement method. Geometric non-linearity is taken into account using the 2nd order theory, while material-induced and temperature-dependent non-linearities are taken into account by means of a cross-sectional analysis in the assembly nodes in the form of a fibre model. The temperature-dependent stress–strain relationships and the thermal strain of structural steel are based on the previously derived calculation values. In terms of stress and heat history the simulation was analogous to the test. This means that after the external loads were applied in the normal temperature range the temperatures of the frame systems

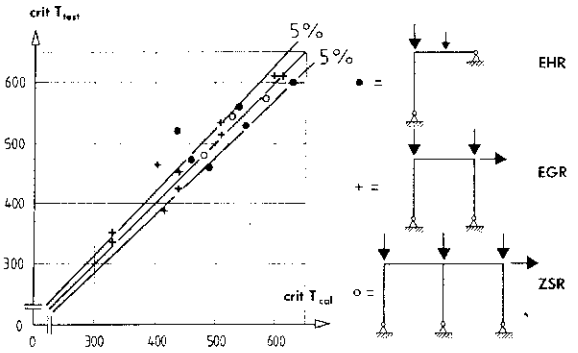

Fig. 8. Comparison between calculated (crit T_{cal}) and measured (crit T_{test}) temperatures of failure.

were gradually increased until failure was reached through loss of stable equilibrium. The temperatures used in the calculation corresponded to those measured in the tests. The theoretical simulation took distributions of residual stresses from Eurocode 3 [14] into account both in determining the load-bearing capacity under normal temperatures to find the load utilization factor and at elevated temperatures.

The peripheral geometries of 18 cross-sections were measured by scanning approximately 30 coordinate pairs in each case. Actual cross-sections were thus determined. For the most important cross-sectional properties the results were very close to the nominal values, with a variation coefficient of less than 1%. Surveying the frame geometry at normal temperature gave maximum angles of the member chord of the columns of approximately 1/600, with average values being much lower. The maximum initial mean deflections of single columns related to column height were in all cases smaller than 1/3000. Column eccentricities and initial curvatures were thus of a negligible magnitude. It was therefore not necessary to take geometric imperfections into consideration in the theoretical investigations.

For all three frame configurations tested the theoretical simulation showed very good agreement with the measured deformations in the entire temperature range from normal temperatures to failure. The calculated temperatures of failure showed good agreement with the results of large-scale model frame tests (Table 2). A comparison of critical temperatures in the test and in the calculation is shown graphically in Fig. 8. Of the 19 tests shown only two lie beyond the 5%

scatter region. In both cases, the calculated result was on the safe side. The deviations are due to particular test conditions, which will not be dealt with here.

It should be pointed out that the calculation values for the temperature-dependent stress–strain relationships, determined on the basis of beams subjected to bending, are equally suitable for the theoretical simulation of frame structures of rolled sections subjected to combined bending and compressive stresses. A detailed description of the load-bearing and deflection behaviour of the frame systems is given in ref. 16.

RECOMMENDATIONS FOR A UNIFORM ASSESSMENT CONCEPT

Given the good correlation between the calculated and experimental results, a generalized concept for single structural elements and frame systems stiffened perpendicular to their plane is recommended as follows.

- The assembly characteristics (geometry, material behaviour, stability effect) are defined by a system slenderness ratio $\bar{\lambda}_{sys}$

$$\bar{\lambda}_{sys} = \sqrt{\frac{\nu_u^I F}{\nu_{ki} F}} = \sqrt{\frac{\nu_u^I}{\nu_{ki}}} \tag{4}$$

The expression under the root sign has the plastic load-bearing capacity in its numerator (e.g., to yield hinge theory, 1st order) and the elastic buckling load of the system in its denominator. Correspondingly, ν_u^I and ν_{ki} are load increasing factors for a given load combination F. (Table 2 gives system slenderness ratios $\bar{\lambda}_{sys}$ for all frame systems tested.)

By analogy with the bar slenderness ratio, the ultimate load-bearing capacity of the cross-section of a single bar is replaced by the plastic load-bearing capacity of the whole structure. The buckling load of the bar is replaced by the elastic buckling load of the whole system (Fig. 9). For a given load combination the plastic limit load and the elastic buckling load can be determined as a multiple of the load using the factors ν_u^I and ν_{ki}. The load quantities F cancel each other out in the radical.

- The external load level is defined by the load utilization factor

$$1/\nu_u = F/F_u \tag{5}$$

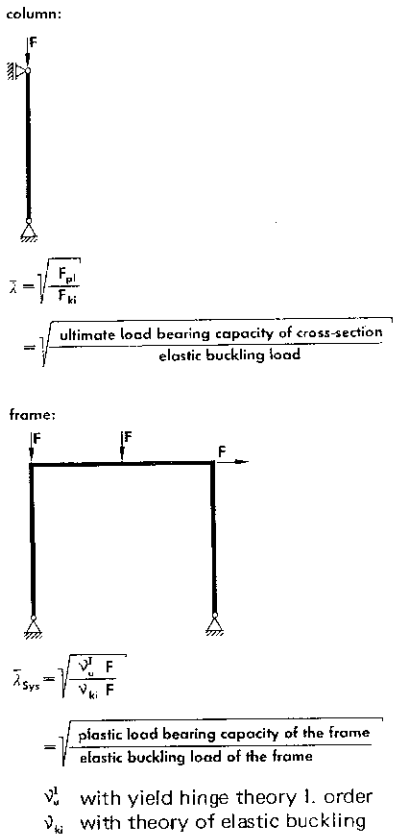

Fig. 9. The characteristic parameters of the proposed design method.

where F_u is the ultimate load at normal temperature taking stability influences into account (e.g., using yield hinge theory) and F is the design load in case of fire action.

- Given uniform heating of the whole system, the critical temperature is a function of F/F_u and $\bar{\lambda}_{sys}$:

$$\text{crit } T = f(F/F_u, \bar{\lambda}_{sys}) \tag{6}$$

For the tests with uniform heating and slenderness ratios of 0.33 (EHR) and 0.93 to 0.96 (EGR) as well as for the calculations with slenderness ratios of 0.33 (EHR) and 0.93 (EGR), the results are summed up in Fig. 10(a) in a representation corresponding to eqn. (6). The lowest critical temperatures were obtained in the medium-slender region ($\bar{\lambda}_{sys} \approx 1$), similar to the pattern with single columns [7]. In addition, the simply supported frames tested were mainly subjected to compression owing to the column loads, and therefore their stability was extremely endangered compared with customary frame assemblies with distributed beam loads. The

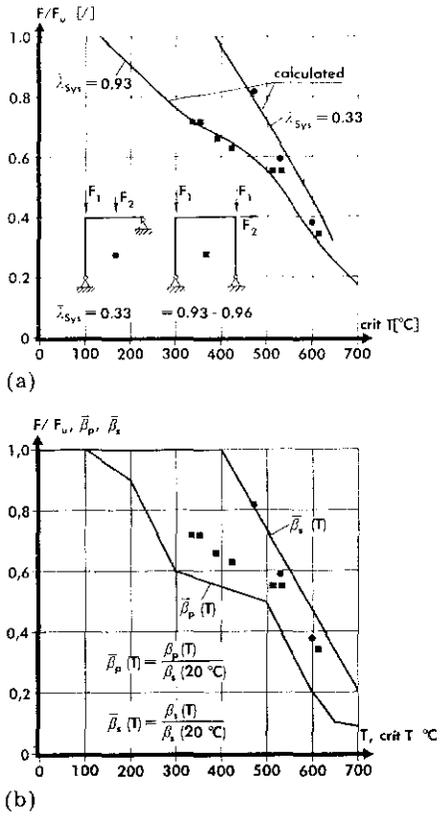

Fig. 10. The measured critical temperatures of the uniformly heated frames in comparison to: (a) the calculation results for $\bar{\lambda}_{sys} = 0.33$ and 0.93; (b) the temperature-dependent elastic limit β_p and yield stress β_s.

curve determined by calculation and confirmed by experiment for load utilization factors between 0.34 and 0.72 can therefore be regarded as the lower critical temperature limit for structural systems in practice.

With lower slenderness ratios, as usually encountered, the critical temperatures rise particularly for high load utilization factors. The upper critical temperature limit is obtained approximately at $\bar{\lambda}_{sys} = 0.33$. Lower slenderness ratios do not increase the critical temperatures because thermally induced constraints increasingly have a depressing effect on the load-bearing capacity.

Worthy of particular note is the overproportionate decrease in the critical temperatures of stability-endangered frames with medium slenderness ratios at high load utilization factors $F/F_u > 0.55$. Figure 10(b) shows the measured temperatures of failure compared with the temperature-dependent progression of the elastic limit $\bar{\beta}_p(T)$ and

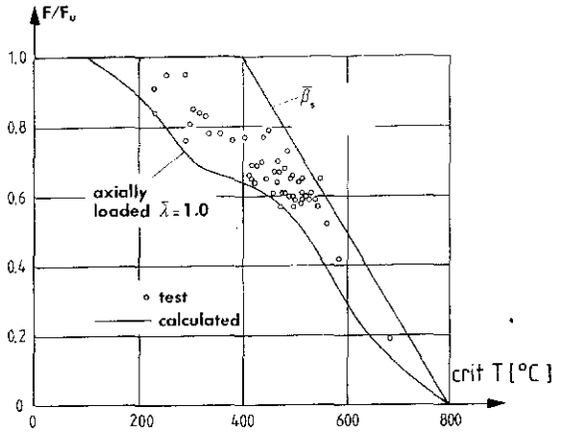

Fig. 11. The measured critical temperatures of over 50 German column tests in comparison to the calculated results for $\bar{\lambda} = 1$ and the temperature-dependent yield point β_s.

the yield point $\bar{\beta}_s(T)$ (see also Fig. 4). It can be seen that the critical temperatures of the frames whose stability is endangered are significantly dependent on the temperature-dependent progression of the elastic limit. In contrast, the two-bar frames with low slenderness ratios fail under the influence of the yield point. For all systems tested, the temperature-dependent yield point represents the upper and the elastic limit the lower estimate of the critical temperatures. The conclusion that can be drawn from this is that at load utilization factors $F/F_u \leqslant 0.5$ failure temperatures of over 500 °C are ensured, even for stability-endangered unbraced frame systems which in comparison with the configurations investigated are not subjected to significantly higher thermal restraint loads. In medium-slender systems ($\bar{\lambda}_{sys} \approx 1$) the region $0.5 < F/F_u \leqslant 0.7$ can be regarded as critical, as even slight deviations in the external loads or a corresponding change in the load utilization factor can lead to substantially different critical temperatures.

The tests carried out additionally — EGR 7/KR and EGR 8/KR with unheated beams and EGR 9/ΔT with a pronounced temperature gradient in the bar — showed no significant effects on the critical temperatures compared with the fully heated systems.

The estimate of the upper and lower limit for the failure temperatures of frame assemblies can equally be applied to single steel columns of rolled sections. Figure 11 shows that for over 50 German full-scale column

fire tests with varying load utilization factors, slenderness ratios, eccentricities, bending axes and section types, for roughly $\bar{\lambda} = \sqrt{F_{pl}/F_{ki}} = 1$, a lower limit can be defined and the temperature-dependent yield point in this paper can be recommended as an upper limit.

ACKNOWLEDGEMENTS

This research work was funded by the Federal Ministry for Research and Technology of the Federal Republic of West Germany and commissioned by Studiengesellschaft für Anwendungstechnik von Eisen und Stahl e.V., Düsseldorf.

LIST OF SYMBOLS

T	temperature of steel assemblies (°C)
$\dot{T}$, $\dot{T}_m$	heating rate and mean heating rate (K/min)
crit T	critical temperature (°C)
F	actual load limit (kN)
F_u	ultimate load-bearing capacity (kN)
F_{pl}	ultimate load-bearing capacity of cross-section (kN)
F_{ki}	elastic buckling load (kN)
M	bending moment (kNm)
A	cross-section (cm^2)
E_0, $\bar{E}_0$	initial Young's modulus (kN/cm^2) and referred initial Young's modulus (/)
w	characteristic displacement (cm)
t	time (min)
h	height of cross-section or geometric length of column (cm)
l	beam length (cm)
x, z	coordinates
σ	stress (kN/cm^2)
ϵ	strain (/)
ϵ_p	elastic limit strain (/)
ϵ_F	yield strain (/)
ϵ_u	ultimate strain (/)
β_p, $\bar{\beta}_p$	elastic limit stress (kN/cm^2) and referred elastic limit stress (/)
β_s, $\bar{\beta}_s$	yield stress (kN/cm^2) and referred yield stress (/)
$\bar{\lambda}_{sys}$	referred system slenderness ratio (/)
$\bar{\lambda}$	referred column slenderness ratio (/)
ν_u^I, ν_{ki}	load increasing factors (/)
$1/\nu_u$	load utilization factor (/)
x, z	coordinates

REFERENCES

1 H. Marx, Grossbrandversuch an einem 3-geschossigen Stahlskelettgebäude, *Symposium Nutzungsgerechtes Bauen im Stahl- und Stahlverbundbau, Dresden, 1975*, IVBH — Berichte der Arbeitskommissionen, Band 21.

2 F. Hoffend, Brandversuche an Stahlrahmen-Versuchsergebnisse, deren Analyse und rechnerische Vergleiche, im Arbeitsbericht 1978 - 80, Teil 1, SFB 148, *Brandverhalten von Bauteilen*, Technische Universität, Braunschweig, 1980.

3 F. Mang and G. Steidl, Zum Brandverhalten von Gesamtkonstruktionen des Stahl- und Stahlverbundbaues, Teil 3: Möglichkeiten und Zielsetzungen der Untersuchung mit Hallen-Kleinmodellen, *Stahlbau, 52* (3) (1983).

4 J. Witteveen, L. Twilt and F. S. K. Bijlaard, The Stability of Braced and Unbraced Frames at Elevated Temperatures, *Preliminary Rep., Second Int. Colloq. on the Stability of Steel Structures, Liège, 1977*, European Convention for Constructional Steelwork (ECCS).

5 R. Beyer and B. Hartmann, Eine Untersuchung des Lastfalles Brand bei Stahlrahmen, in *Finite Elemente in der Baupraxis*, Verlag W. Ernst und Sohn, Berlin, 1978.

6 U. Quast, R. Hass and K. Rudolph, *STABA-F, A Computer Program for the Determination of Load-Bearing and Deformation Behaviour of Uni-Axial Structural Elements under Fire Action*, Technische Univeristät, Braunschweig, March, 1984.

7 F. Hoffend, *Calculation of Critical Temperatures of Fire-exposed Steel Columns*, Technische Universität, Braunschweig, 1984.

8 A. Rubert, Experimentelle Untersuchungen zum Brandverhalten kompletter, ebener Rahmensysteme aus Baustahl, *Forschungsbericht zur Teilaktivität 3.2 des Vorhabens Bau 6004/P86, Teil I (Bericht), Teil II (Dokumentation)*, Studiengesellschaft für Anwendungstechnik von Eisen und Stahl e.V., Düsseldorf, durchgeführt im Krupp Forschungsinstitut, Essen, 1984.

9 K. Roik and P. Schaumann, Berechnung des Brandfall Tragverhaltens von Hauptrahmentragwerken kompletter Bauwerkssysteme, *Forschungsbericht zur Teilaktivität 3.3 des Vorhabens Bau 6004/P86*, Studiengesellschaft für Anwendungstechnik von Eisen und Stahl e.V., Düsseldorf, durchgeführt im Institut für Konstruktiven Ingenieurbau II der Ruhr-Universität Bochum, 1984.

10 A. Rubert, Die Grossmodelltechnik, ein neuartiger Weg für Serienuntersuchungen zum Brandverhalten von Einzelbauteilen und Gesamtkonstruktionen mit quantifizierbarem Aussagewert. Technische Mitteilungen Krupp, Forschungsberichte, Heft 2, Band 41, 1983.

11 *DIN 4102, Brandverhalten von Baustoffen und Bauteilen*, März, 1981.

12 EKS Kommission, *European Recommendations for the Fire Safety of Steel Structures*, Elsevier, Amsterdam, 1983.

13 P. Schaumann, Zur Berechnung stählerner Bauteile und Rahmentragwerke unter Brandbeanspruchung, Technisch-wissenschaftliche Mitteilungen Nr. 84-4, *Dissertation,* Institut für Konstruktiven Ingenieurbau, Ruhr-Universität Bochum, 1984.
14 Commission of the European Communities, *Eurocode No. 3, Common Unified Rules for Steel Structures, Report EUR 8849*, DE, EN, FR, 1984.
15 A. Rubert and P. Schaumann, Temperaturabhängige Werkstoffeigenschaften von Baustahl bei Brandbeanspruchung, *Stahlbau*, (3) (1985).
16 A. Rubert and P. Schaumann, Tragverhalten stählerner Rahmensysteme bei Brandbeanspruchung, *Stahlbau*, (9) (1985).